Electronic Supplementary Information for

Synthesis, characterization, and atropisomerism of iron complexes containing the *tetrakis*(2-chloro-6-fluorophenyl)porphyrinate ligand

Daniel J. Meininger, Nicanor Muzquiz, Hadi D. Arman, and Zachary J. Tonzetich*

Department of Chemistry, University of Texas at San Antonio, San Antonio, TX 78249
zachary.tonzetich@utsa.edu

Contents

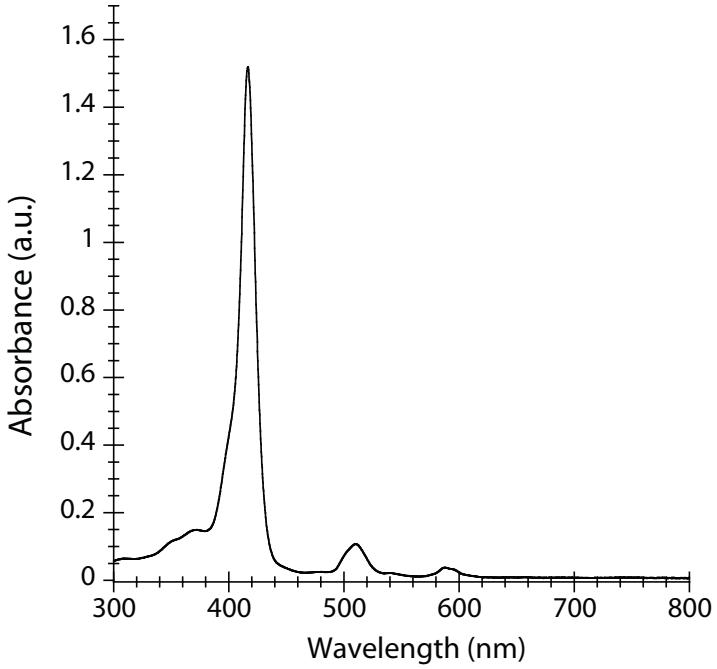

Figure S1. Electronic absorption spectrum of H_2(ClFTPP) in dichloromethane.

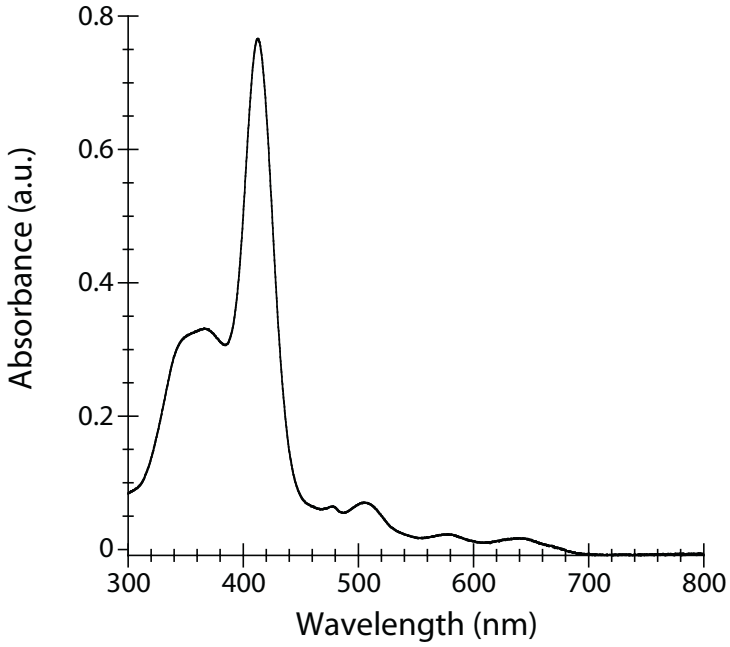

Figure S2. Electronic absorption spectrum of [FeCl(ClFTPP)] in dichloromethane.

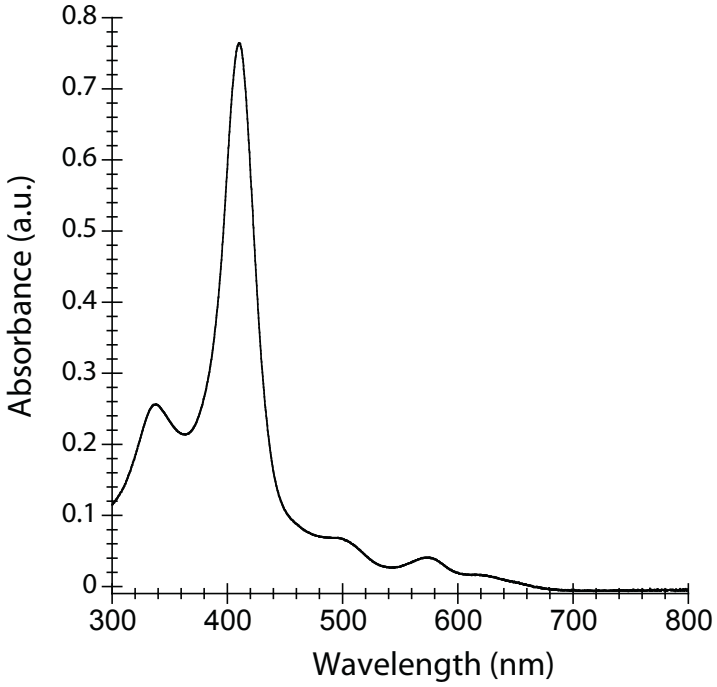

Figure S3. Electronic absorption spectrum of [Fe(OAc)(ClFTPP)] in dichloromethane.

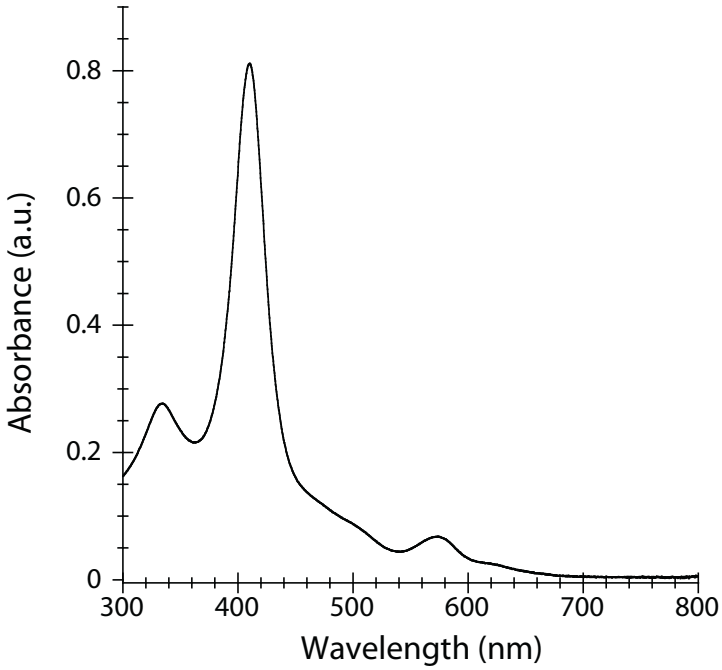

Figure S4. Electronic absorption spectrum of [Fe(OH)(ClFTPP)]·H_2O in dichloromethane.

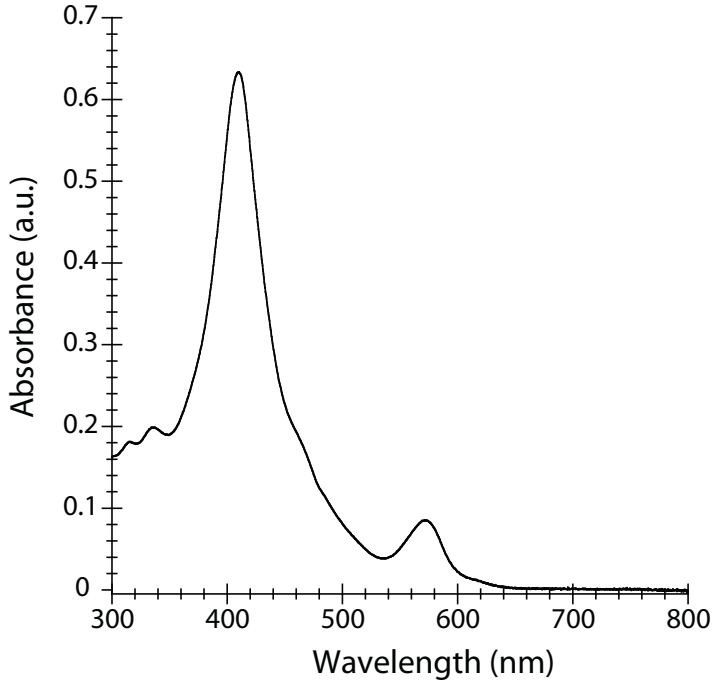

Figure S5. Electronic absorption spectrum of [Fe(OMe)(ClFTPP)] in dichloromethane.

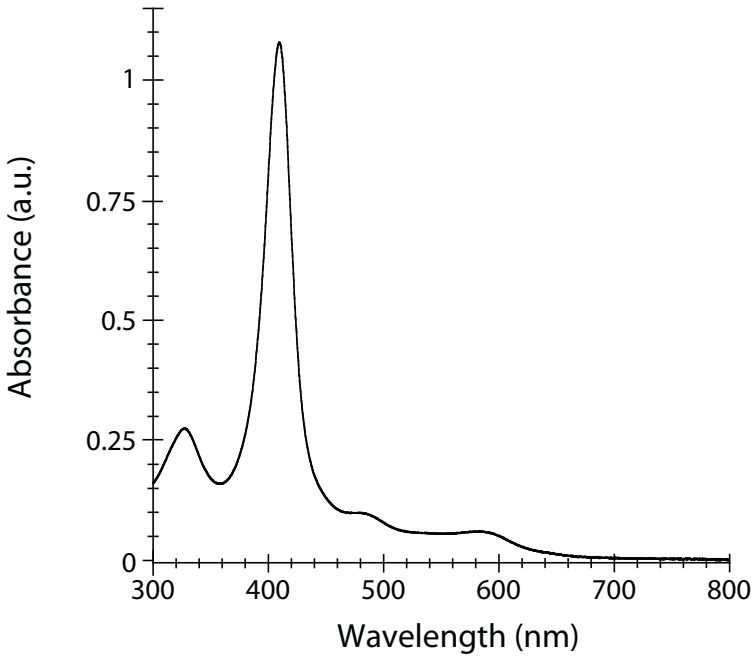

Figure S6. Electronic absorption spectrum of [Fe(O-2-$NH_2C_6H_4$)(ClFTPP)] in dichloromethane.

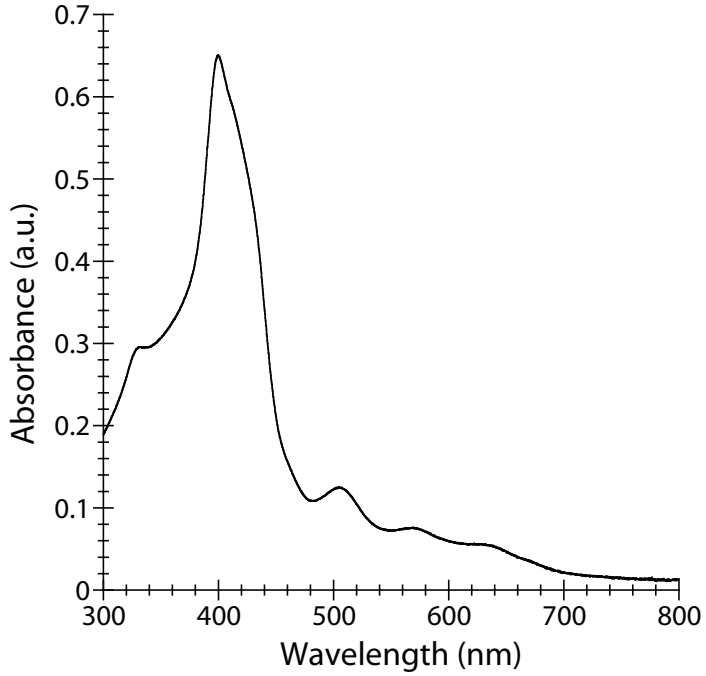

Figure S7. Electronic absorption spectrum of [Fe(STIPS)(ClFTPP)] in dichloromethane.

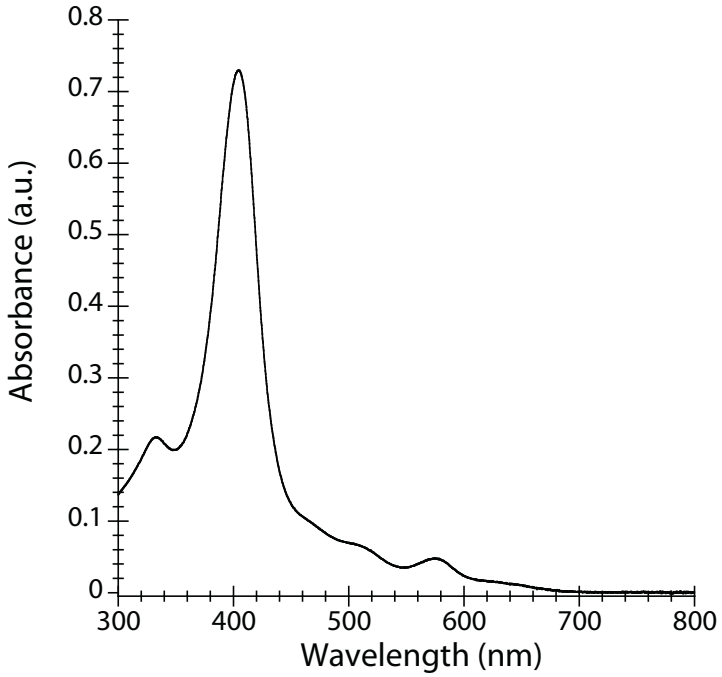

Figure S8. Electronic absorption spectrum of $[Fe(OH_2)_2(ClFTPP)](ClO_4)$ in dichloromethane.

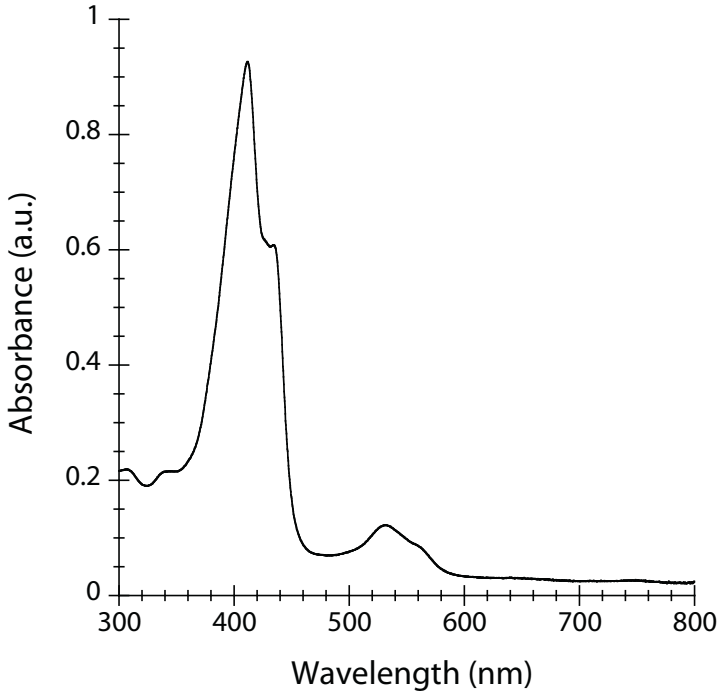

Figure S9. Electronic absorption spectrum of [Fe^{II}(ClFTPP)] in dichloromethane.

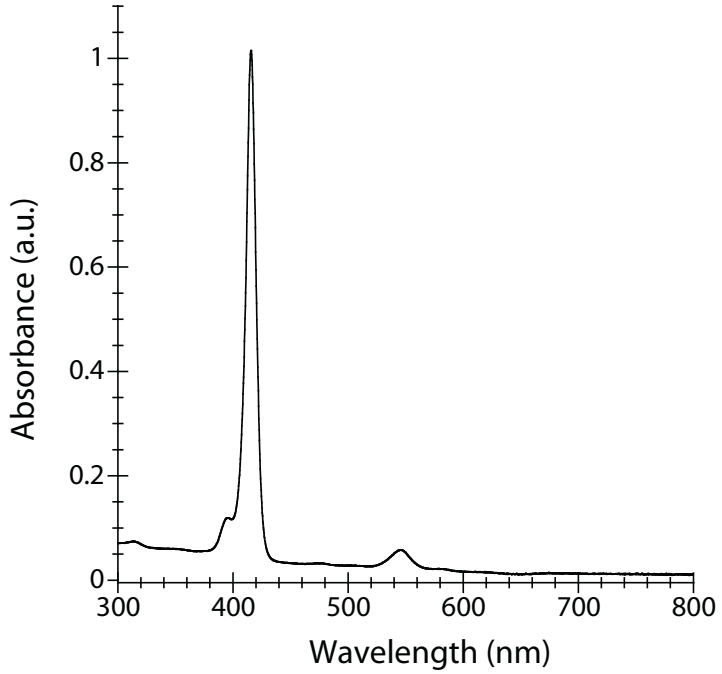

Figure S10. Electronic absorption spectrum of [Zn(ClFTPP)] in dichloromethane.

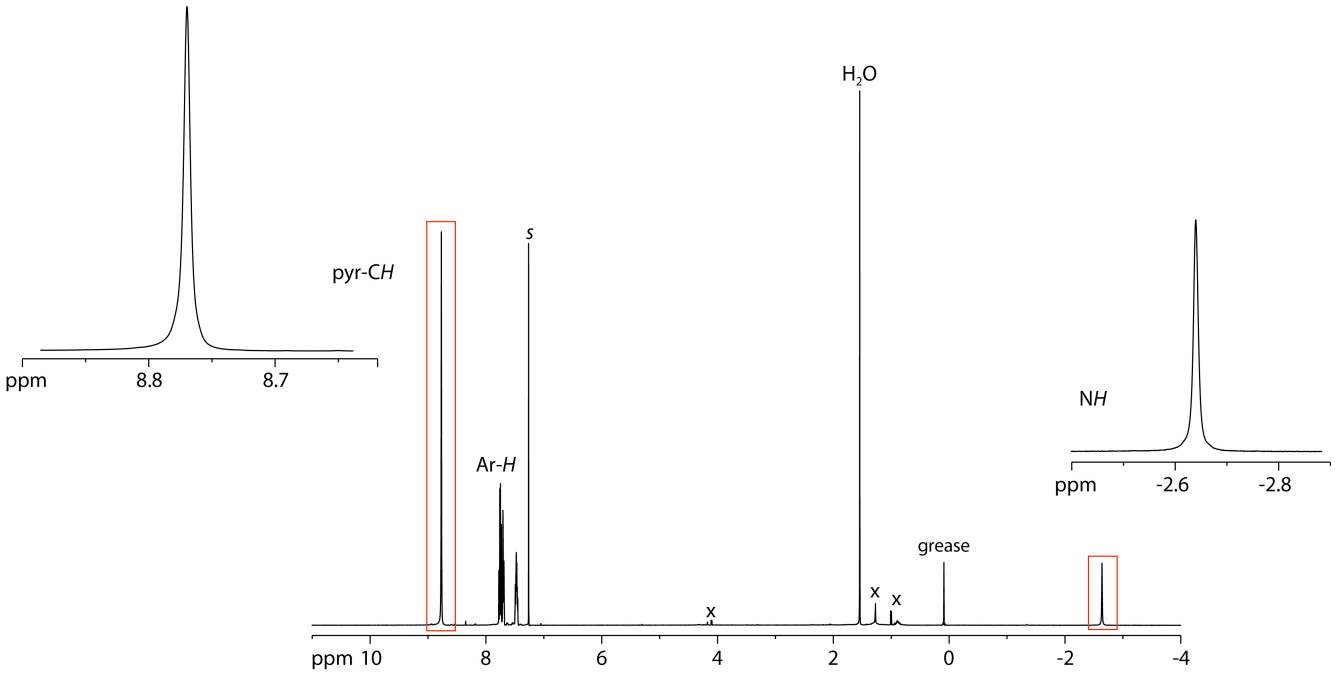

Figure S11. 500 MHz ^{1}H NMR spectrum of H_2(ClFTPP) in chloroform-*d*. Insets display peaks corresponding to the pyrolic hydrogen atoms (both N*H* and C*H*).

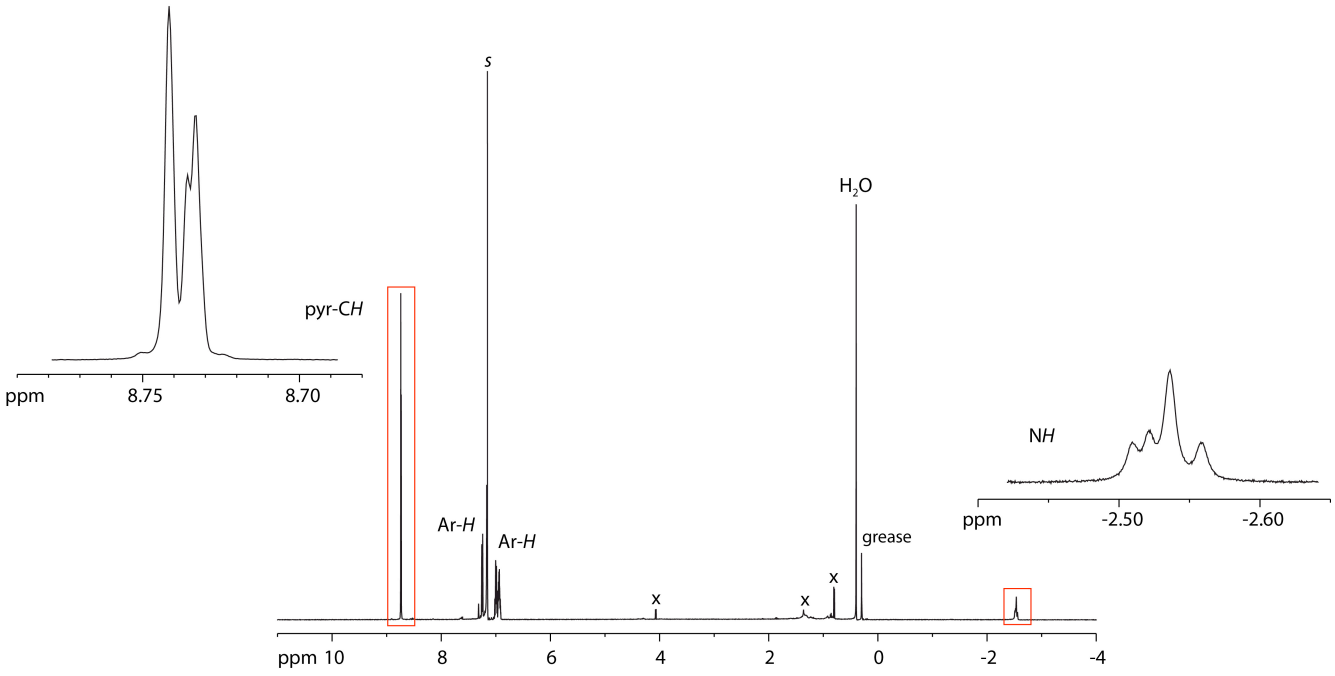

Figure S12. 500 MHz ^{1}H NMR spectrum of H_2(ClFTPP) in benzene-d_6. The insets display peaks corresponding to the pyrolic hydrogen atoms (both N*H* and C*H*).

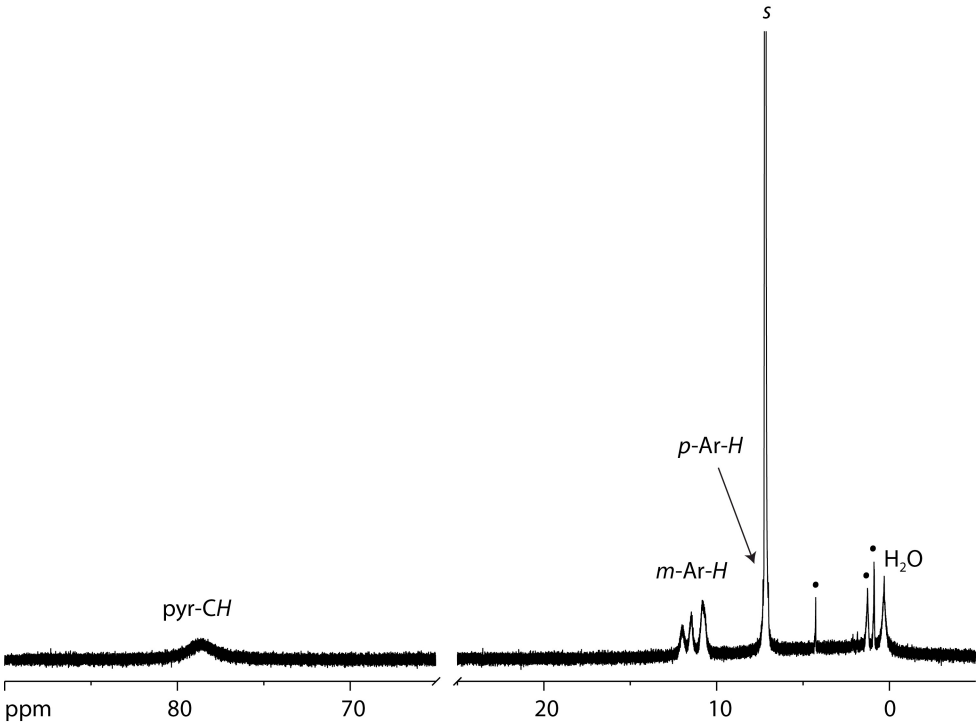

Figure S13. 500 MHz ^{1}H NMR spectrum of [Fe(O_2CCH_3)(ClFTPP)]·H_2O in benzene-d_6. Black dots denote resonances due to pentane and dichloromethane.

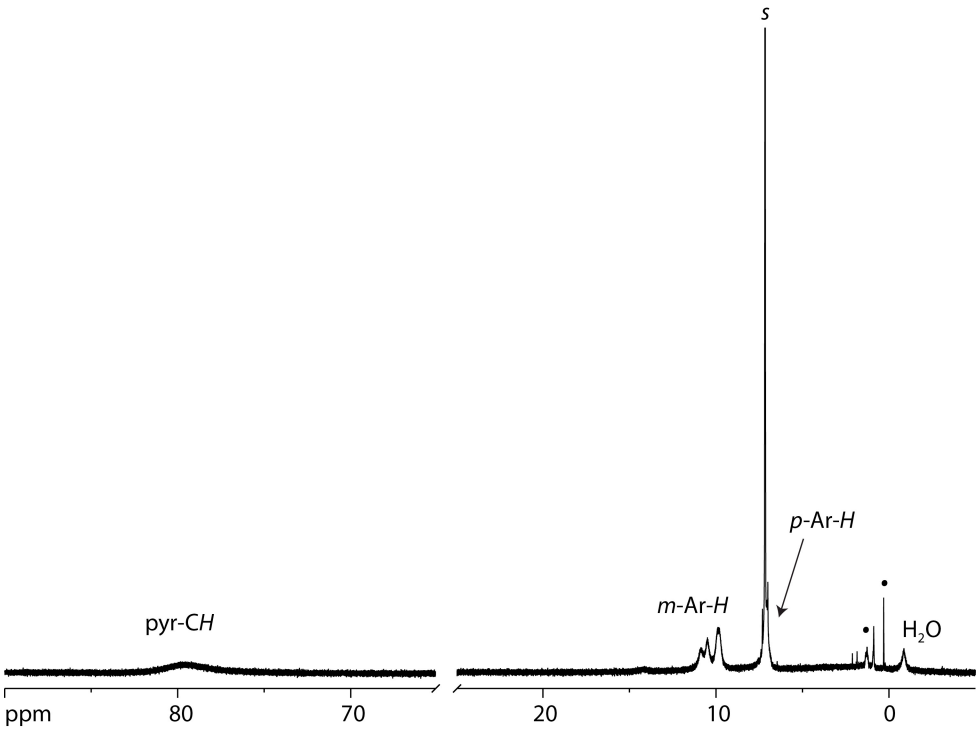

Figure S14. 500 MHz ^{1}H NMR spectrum of [Fe(OH)(ClFTPP)]·H_2O in benzene-d_6. Black dots denote resonances due to pentane and silicon grease.

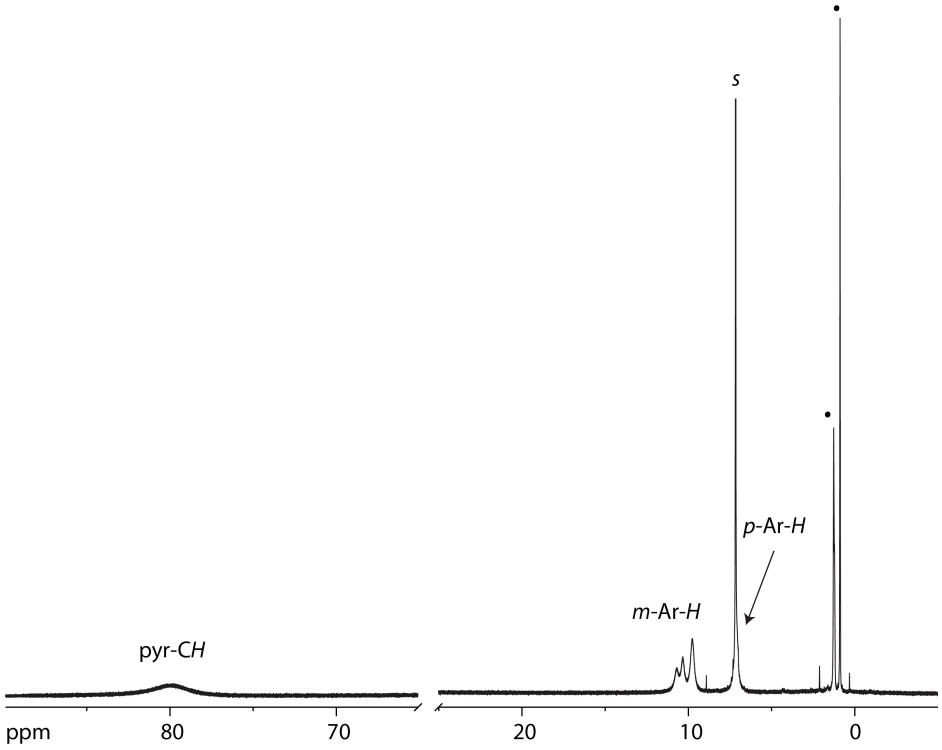

Figure S15. 500 MHz ^{1}H NMR spectrum of [Fe(OMe)(ClFTPP)] in benzene-d_6. Black dots denote resonances due to pentane.

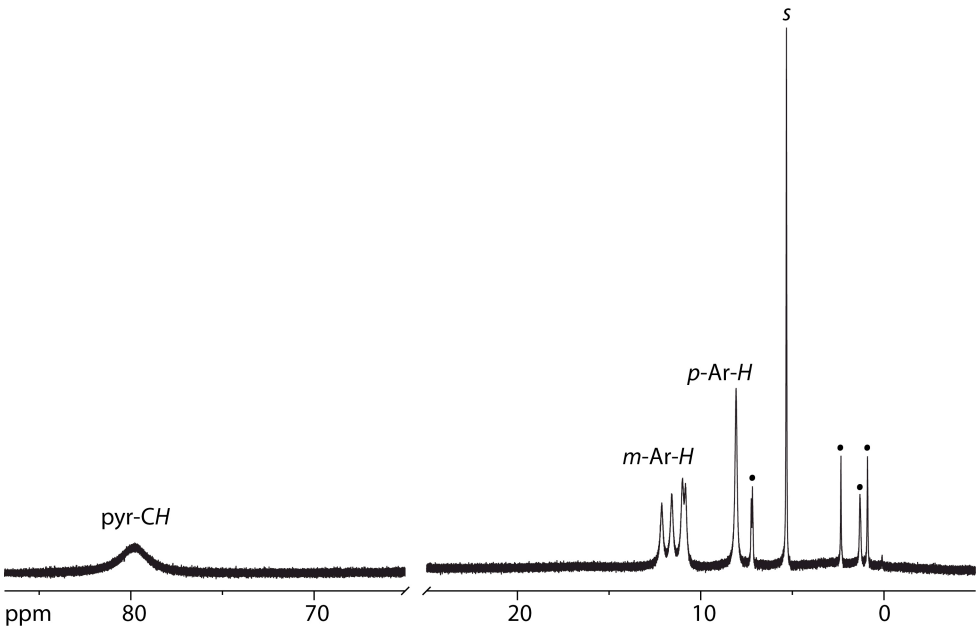

Figure S16. 500 MHz ^{1}H NMR spectrum of [Fe(O-2-$NH_2C_6H_4$)(ClFTPP)] in methylene chloride-d_2. Black dots denote resonances due to pentane and toluene.

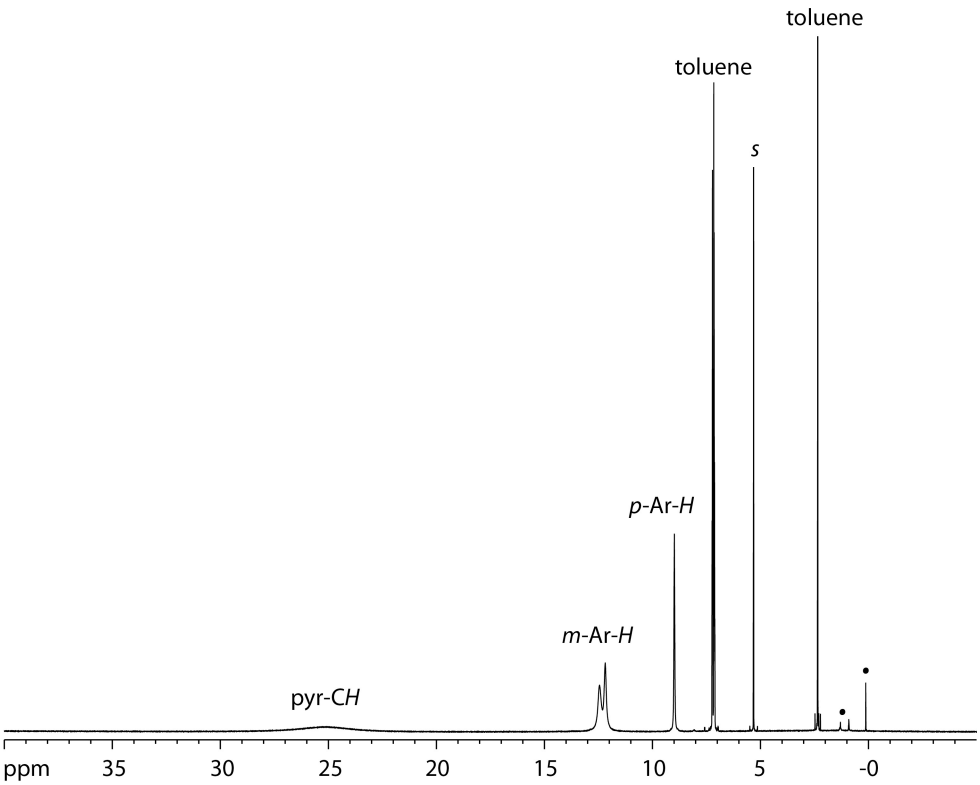

Figure S17. 500 MHz ^{1}H NMR spectrum of $[Fe(OH_2)_2(ClFTPP)](ClO_4)$·toluene in dichloromethane-d_2. Black dots denote resonances due to pentane and grease.

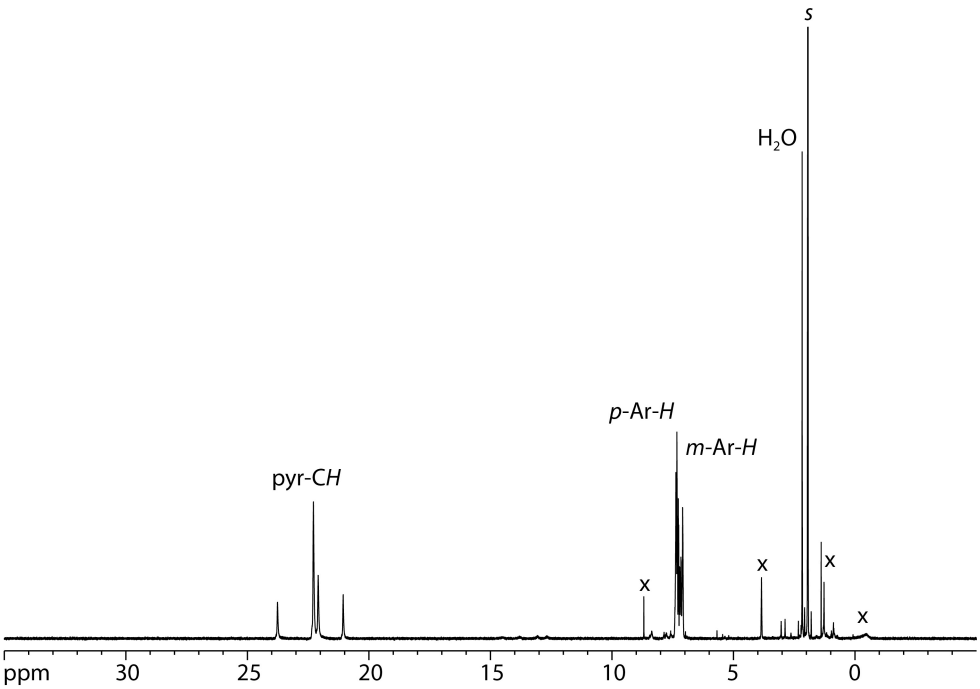

Figure S18. 500 MHz ^{1}H NMR spectrum of [Fe(ClFTPP)] in acetonitrile-d_3. Note that slow decomposition of the compound is observed to occur in this solvent accounting for the multitude of unassigned peaks.

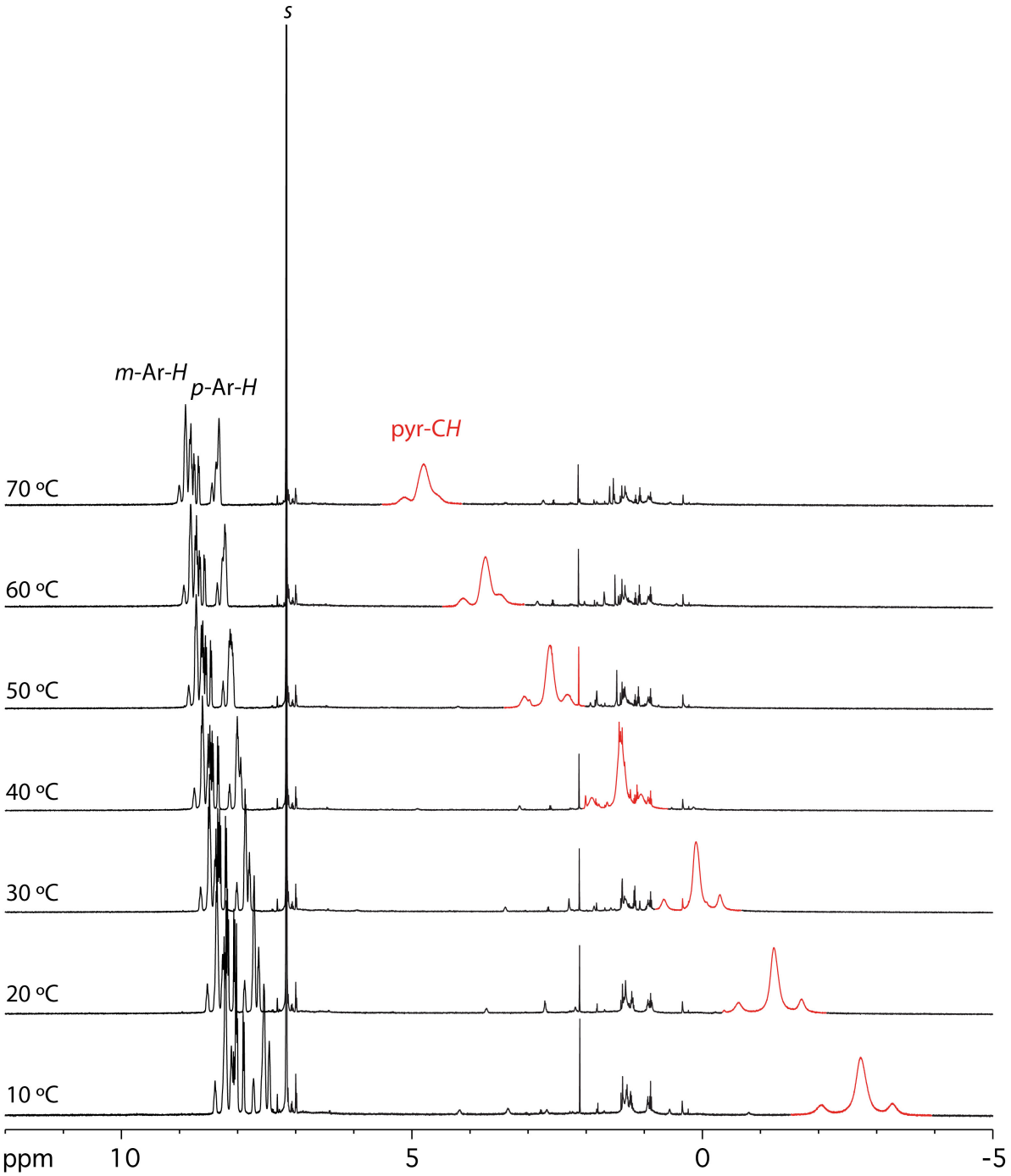

Figure S19. 500 MHz ^{1}H NMR spectrum of [Fe^{II}(ClFTPP)] in benzene-d_6 between 10 and 80 °C. The pyrrolic-C*H* resonance is highlighted in red.

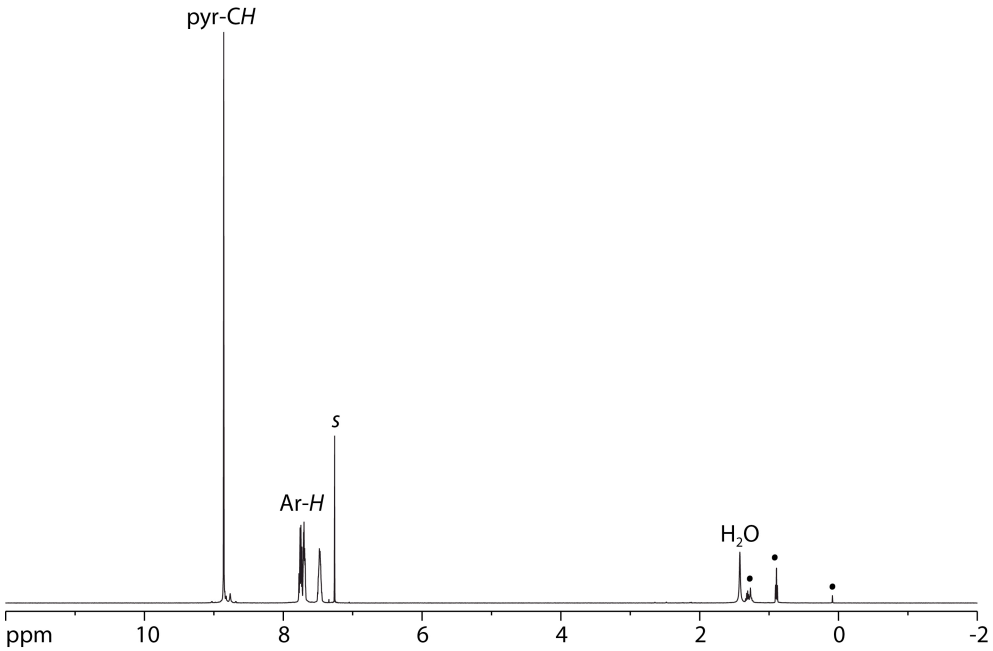

Figure S20. 500 MHz ^{1}H NMR spectrum of [Zn(ClFTPP)] in chloroform-*d*. Black dots denote resonances due to pentane and silicon grease.

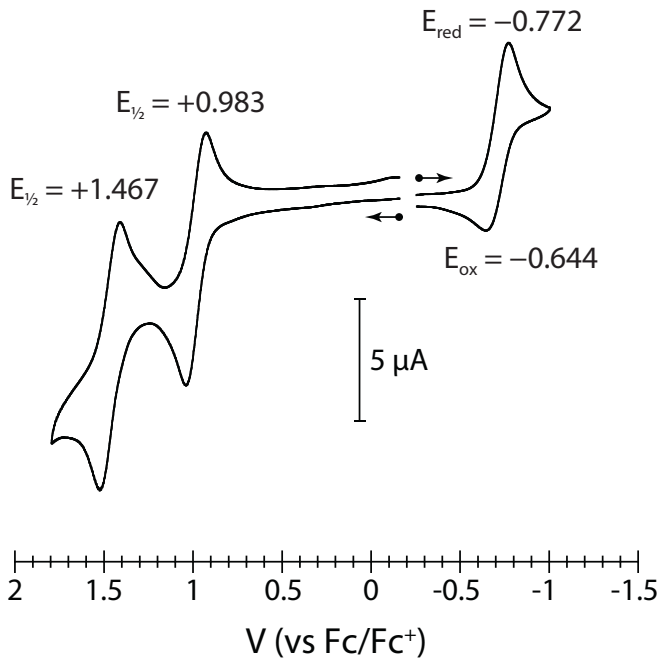

Figure S21. Cyclic voltammogram of 2 mM [FeCl(ClFTPP)] at a platinum electrode in methylene chloride. Scan rate is 50 mV/s and the supporting electrolyte is 0.1 M Bu_4NPF_6.

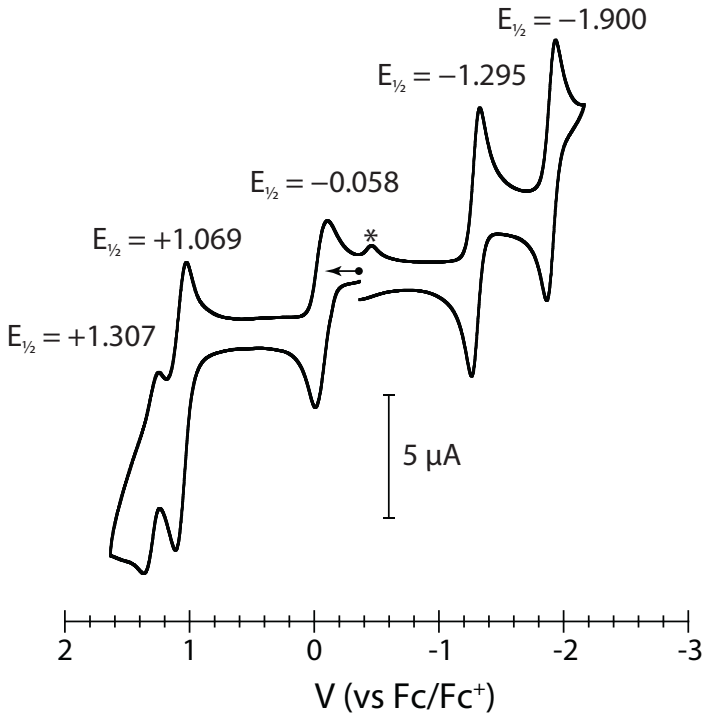

Figure S22. Cyclic voltammogram of 2 mM [Fe^{II}(ClFTPP)] at a platinum electrode in acetonitrile. Scan rate is 50 mV/s and the supporting electrolyte is 0.1 M Bu_4NPF_6. Asterisk denotes unknown species formed during the electrode processes or by decomposition of the compound in acetonitrile.

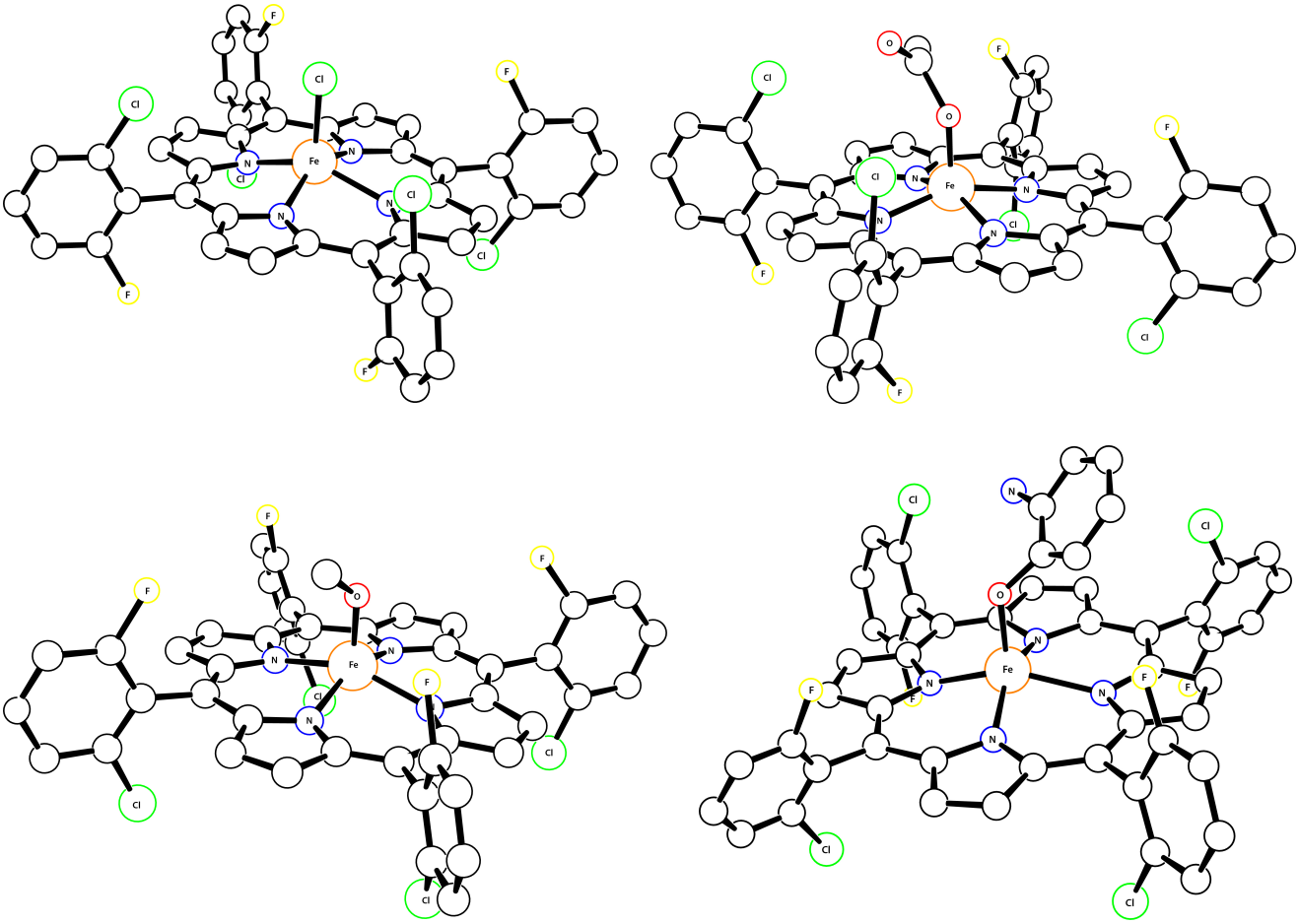

Figure S23. Renderings of the solid-state structures of [FeCl(ClFTPP)], [Fe(OAc)(ClFTPP)], [Fe(OMe)(ClFTPP)], and [Fe(O-2-$NH_2C_6H_4$)(ClFTPP)] from crystallographic data. Note that the structures contain significant disorder in the 2,6-chlorofluorophenyl rings and could not be solved completely. The images above are only provided to demonstrate connectivity of the porphyrin core, not the orientation of the *meso*-aryl rings.

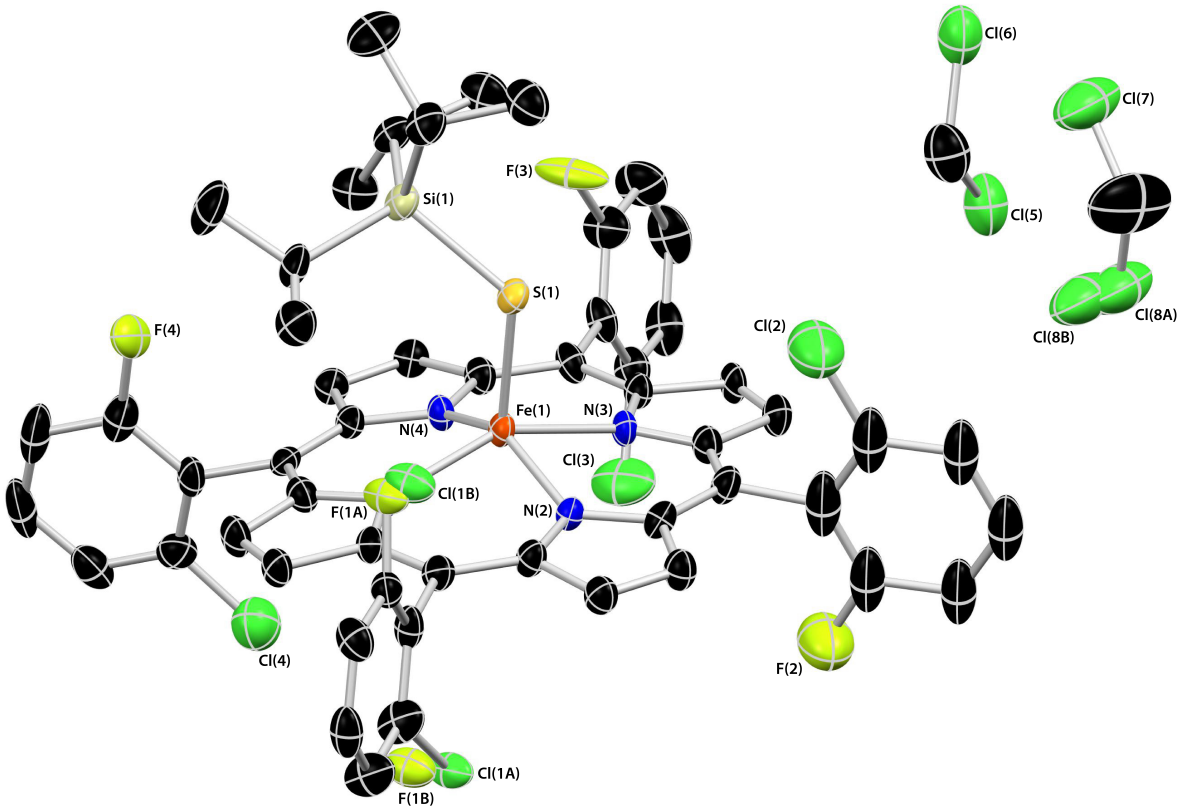

Figure S24. Thermal ellipsoid rendering (50%) of [Fe(SSi^{i}Pr$_3$)(ClFTPP)]·$(CH_2Cl_2)_3$ showing components of the modeled disorder. A third CH_2Cl_2 molecule could not be refined and was removed using SQUEEZE.

Table 1. Crystallographic data and refinement parameters for [Fe(SSi^{i}Pr$_3$)(ClFTPP)].‡

Compound	**[Fe(SSi^{i}Pr$_3$)(ClFTPP)]**
Empirical formula	$C_{53}H_{41}Cl_4F_4FeN_4SSi\cdot(CH_2Cl_2)_2$
Formula weight (g/mol)	1237.55
Temperature (K)	98(2)
Crystal system, space group	Monoclinic $P2_1$
Unit cell dimensions (Å, deg)	a = 11.785(2) b = 21.887(4) c = 12.845(2) β = 117.1275(19)°
Volume (Å^3)	2948.7(9)
Z	2
Calculated density (g/cm^3)	1.394
Absorption coefficient (mm^{-1})	0.726
F(000)	1262
Crystal size (mm)	0.40 × 0.25 × 0.10
Θ range	2.58 to 25.05º
Limiting indices	−14 ≤ h ≤ 12, −26 ≤ k ≤ 18, 0 ≤ l ≤ 15
Reflections collected / unique	7729 / 7729 [R_{int} = 0.0346]
Completeness to Θ	99.0%
Absorption correction	multi-scan ABSCOR
Min. and max transmission	0.626 and 1.000
Data / restraints / parameters	7729 / 1 / 618
Goodness-of-fit on F^2	1.008
Final R indices [I > 2σ(I)]	R_1 = 0.0685, wR_2 = 0.1520
R indices (all data)	R_1 = 0.0722, wR_2 = 0.1545
Largest diff. peak and hole (e·Å^{-3})	1.506 and −0.775
Absolute Structure Parameter	−0.03(3)

‡Refinement method was full-matrix least-squares on F^2; wavelength = 0.71073 Å. $R_1 = \sum||F_o|-|F_c||/\sum|F_o|$; $wR_2 = \{\sum[w(F_o^2-F_c^2)^2]/\sum[w(F_o^2)^2]\}^{½}$.